

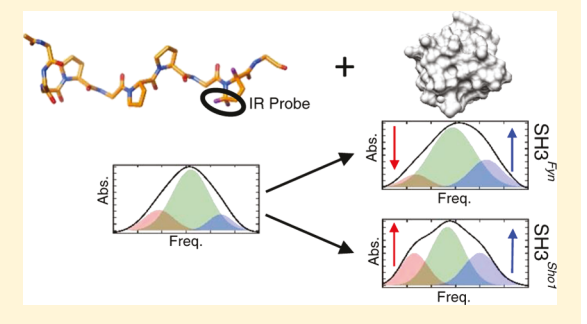
# Involvement of Local, Rapid Conformational Dynamics in Binding of Flexible Recognition Motifs

Gregory S. Bukowski, Rachel E. Horness, and Megan C. Thielges\*

Department of Chemistry, Indiana University, Bloomington, Bloomington, Indiana 47405, United States

Supporting Information

ABSTRACT: Flexible protein sequences populate ensembles of rapidly interconverting states differentiated by small-scale fluctuations; however, elucidating whether and how the ensembles determine function experimentally is challenged by the combined high spatial and temporal resolution needed to capture the states. We used carbon-deuterium (C–D) bond vibrations incorporated as infrared probes to characterize with residue-specific detail the heterogeneity of states adopted by proline-rich (PR) sequences and assess their involvement in recognition of Src homology 3 domains. The C-D absorption envelopes provided evidence for two or three sub-populations at all proline residues. The changes in the subpopulations induced by binding generally reflected



recognition by conformational selection but depended on the residue and the state of the ligand to illuminate distinct mechanisms among the PR ligands. Notably, the spectral data indicate that greater adaptability among the states is associated with reduced recognition specificity and that perturbation to the ensemble populations contributes to differences in binding entropy. Broadly, the study quantifies rapidly interconverting ensembles with residue-specific detail and implicates them in function.

# **■ INTRODUCTION**

Inherently flexible, disordered sequences often mediate protein-protein interactions that underlie signaling and other critical functions of a cell.<sup>1,2</sup> As such sequences can exist as dynamic ensembles, knowledge of the heterogeneity of populated states and their dynamics is central to understanding function. While the functional importance of large-scale conformational changes has become well accepted, many protein dynamics can be small in scale and rapid in timescale, and their role is less well established. All residues of all proteins possess local rapid dynamics but not all are critical to function. Nevertheless, such motions are likely consequential for flexible, disordered sequences. Even for structured proteins, NMR relaxation methods have demonstrated that conformational entropy changes are often dominated by the rapid, local motion of protein side chains.3

Part of the hindrance to elucidating the functional role of local, rapidly interconverting states arises from the challenge of characterizing the ensembles to elucidate exactly their involvement. No one experimental approach is likely to afford sufficient spatial and temporal resolution to resolve all potentially important states. NMR spectroscopy is one of the most powerful approaches for gaining molecular-level information about flexible protein sequences,<sup>4,5</sup> but often the ensembles interconvert fast on the NMR timescale, so they remain difficult to fully capture. Other approaches, such as circular dichroism (CD) spectroscopy, small-angle X-ray scattering, and dynamic light scattering, provide only global views.<sup>6-8</sup> We have explored the use of site-specific infrared

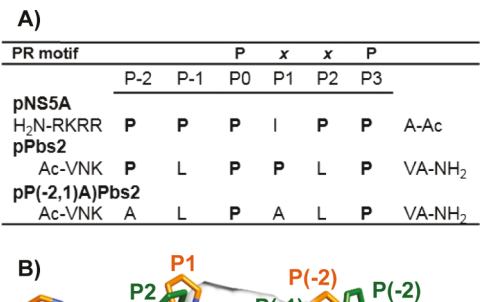
(IR) spectroscopy to characterize proline-rich (PR) sequences found in disordered regions of proteins and demonstrated the possibility to resolve rapidly interconverting states with residue-specific detail. Through expansion of the studies to several PR sequences and their recognition of two Src homology 3 (SH3) domains, we now provide evidence to support that these states play a role in the specificity and thermodynamics of molecular recognition.

IR spectroscopy provides bond-specific spatial resolution with an inherently fast timescale for directly capturing even the most rapidly interconverting states. To overcome the issue of spectral congestion in protein IR spectra, chemical functional groups with vibrational frequencies well separated from those of the native protein, within the "transparent window" around 1900-2300 cm<sup>-1</sup>, can be incorporated at specific locations in proteins. 10-12 The spectral selectivity makes possible detection of absorptions of single vibrations in proteins to provide a reporter local to the site. A number of such frequency-resolved probes are in widespread use, including nitrile, azide, and alkyne groups, but they introduce unnatural moieties. 13-16 In contrast, carbon-deuterium (C-D) bonds provide virtually non-perturbative reporters of the bonds of the protein itself. While comparatively underutilized, C-D probes have been used to investigate enzyme catalysis, folding, and protein recognition.  $^{18-22}\,$ 

Received: July 23, 2019 Revised: September 18, 2019 Published: September 19, 2019

8387

We have taken advantage of C–D vibrational probes for measuring the local environments and dynamics of PR sequences toward developing a more complete molecular understanding of their binding to SH3 domains, which have served as a paradigm system for the study of recognition specificity. PR and other linear recognition motifs are generally enriched in disordered regions of proteins. The PR motif of SH3 domains contains a consensus sequence PxxP, where x is typically a hydrophobic amino acid and a positively charged residue one or two positions away. (Consensus numbering for residues of the PR motif is provided in Figure 1a). In structures of the complexes with



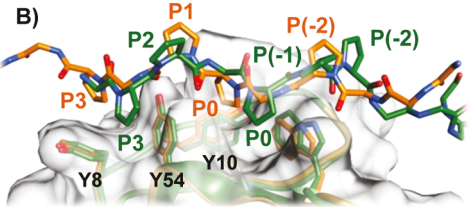


**Figure 1.** (A) Consensus numbering for the PR ligands investigated in this study. (B) Average structures of pNS5A (green) and pPbs2 (orange) bound to SH3<sup>Fyn</sup> from MD simulations. Proline in the PR ligands are numbered based on the consensus in (A). The side chains are shown for the conserved tyrosine residues of the binding pocket in SH3<sup>Fyn</sup>.

SH3 domains, the PR ligands adopt the polyproline type II (PPII) secondary structure. The backbone forms an elongated left-handed-helix with three-fold symmetry that places the motif prolines in register to pack within grooves formed by a set of conserved aromatic residues of the SH3 domain (Figure 1b).<sup>29,30</sup> The displacement of water molecules in such a hydrophobic interaction should be entropically favorable, but experimental studies typically find the binding entropically unfavorable, <sup>31–33</sup> indicating that the restriction of dynamics of the PR ligand, SH3 domain, and/or associated solvent accompany their association.

To begin to unravel how dynamics contribute to the mechanisms of recognition of PR sequences and SH3 domains, we have focused as a model system on the PR sequence of the kinase Pbs2 (pPbs2) and the SH3 domain from osmosensor protein Sho1 (SH3<sup>Sho1</sup>). SH3<sup>Sho1</sup> and pPbs2 participate in a specific interaction within the yeast proteome to mediate the high osmolarity stress response pathway; previous studies have found that no other yeast SH3 domain can functionally complement SH3<sup>Sho1</sup>. In prior studies, we introduced ( $C_{\alpha}$ - $d_{\gamma}$ - $C_{\delta}$ - $d_{2}$ )-proline ( $d_{3}$ Pro) at motif residues P0 and P3 of pPbs2 and used the C-D vibrations to characterize the association with SH3<sup>Sho1</sup>. We observed multiple IR absorption bands for individual modes of the  $C_{\delta}$ D<sub>2</sub> bonds, which indicated that the bonds experience multiple environments or that the labeled residues adopt an ensemble of subpopulations. Moreover, NMR spectroscopy of the pPbs2 peptide labeled at the same

bonds with <sup>13</sup>C showed no evidence for multiple resonances, implying that the states uncovered by IR spectroscopy interconvert rapidly on the NMR timescale.

We then undertook a more systematic investigation employing a total of 11 C–D probes introduced at all proline residues in pPbs2 and two other PR ligands (Figure 1a). In addition to pPbs2, this study included a peptide with the pPbs2 sequence, but the two nonmotif prolines mutated to alanine, p(P(-2,1)A)Pbs2. The third ligand characterized, pNS5A from the nonstructural protein 5A of hepatitis C virus, has a high proline content, with proline at five of the six residues encompassing the PR motif. All C–D probes showed multiple absorption bands associated with single vibrational modes, providing additional evidence for the presence of multiple subpopulations at the proline residues in PR ligands.

While we had detected multiple subpopulations at residues throughout PR sequences, we did not establish whether and how the states contributed to molecular recognition. Toward addressing this question, we now have analyzed each of the proline residues of the PR ligands in complexes with SH3 domains for comparison to the free states. We re-evaluated the recognition of pPbs2 with the physiological partner SH3<sup>Sho1</sup> and compared it with a second SH3 domain, a subunit of human Fyn tyrosine kinase (SH3<sup>Fyn</sup>). Although a human protein, SH3<sup>Fyn</sup> can reconstitute SH3<sup>Sho1</sup> function.<sup>34</sup> We also compared the complexes of both domains with the mutated sequence of pPbs2, p(P(-2,1)A)Pbs2. Unlike pPbs2, p(P-(-2,1)A)Pbs2 shows cross-reactivity among yeast SH3 domains, and moreover, the recognition promiscuity leads to a fitness defect.<sup>34</sup> Finally, we characterized the recognition of SH3<sup>Fyn</sup> and pNS5A, which bind with high affinity.<sup>35</sup> The ligands pPbs2/p(P(-2,1)A)Pbs2 and pNS5A, so-called type 1 and 2 ligands, respectively, also bind SH3<sup>Fyn</sup> in opposite orientation with respect to their N- and C-termini (Figure 1).30 To provide additional insights into the bound structures, molecular dynamics (MD) simulations were performed for the complexes with SH3<sup>Fyn</sup>, complementing our prior study of the free ligands. Further, the binding reactions were characterized by isothermal titration calorimetry (ITC) to assess potential differences in the binding thermodynamics. The IR spectra provided residue-specific experimental information about the subpopulations along the PR ligands to illuminate distinct binding mechanisms. Moreover, in combination, the data support that the dynamic ensemble likely contributes to the thermodynamics and specificity of recognition.

# **MATERIALS AND METHODS**

Expression and Purification of SH3 Domains. A plasmid was generously provided by Catherine Pallen (University of British Columbia) for expression of SH3<sup>Fyn</sup> as a GST-tagged construct with a glycine linker separated by a thrombin cleavage site. SH3<sup>Fyn</sup> was expressed in *Escherichia coli* BL21(DE3), isolated via affinity chromatography, digested with thrombin, and further purified via size exclusion chromatography, as described in detail in Supporting Information. The expression plasmid for SH3<sup>Sho1</sup> was kindly provided by Alan Davidson (University of Toronto). Expression and purification of SH3<sup>Sho1</sup> were performed as previously reported.<sup>22</sup>

**Peptide Synthesis.** Peptides with sequences Ac-VNKPLPPLPVA-NH<sub>2</sub> (pPbs2), Ac-VNKALPALPVA-NH<sub>2</sub> (p-(P(-2,1)A)Pbs2), and Ac-APPIPPPRRKR-NH<sub>2</sub> (pNS5A) were synthesized by fluorenylmethoxycarbonyl solid-phase

peptide synthesis as previously reported. N- and C-termini were acetylated and amidated, respectively. In total, 14 peptides were prepared: one unlabeled variant of each peptide and variants with  $(C_{\alpha}$ -d,  $C_{\delta}$ - $d_2$ )-proline incorporated at each of the proline residues in each peptide, P(-2), P(-1), P(-

Fourier Transform Infrared Spectroscopy. Peptide and protein concentrations were determined by UV/vis absorbance spectroscopy (pPbs2  $\varepsilon_{205} = 43318.56 \text{ M}^{-1} \text{ cm}^{-1}$ ; p(P(-2,1)-A)Pbs2  $\varepsilon_{205} = 40737.27 \text{ M}^{-1} \text{ cm}^{-1}$ ; pNS5A  $\varepsilon_{220} = 17450 \text{ M}^{-1} \text{ cm}^{-1}$ ; SH3<sup>Fyn</sup>  $\varepsilon_{280} = 16960 \text{ M}^{-1} \text{ cm}^{-1}$ ; SH3<sup>Sho1</sup>  $\varepsilon_{280} = 18450 \text{ M}^{-1} \text{ cm}^{-1}$ ). Peptide concentrations were adjusted to 4 mM in 50 mM sodium phosphate, pH 7.0, 100 mM NaCl. To characterize the SH3 domain-peptide complexes, samples were prepared containing 4 mM peptide and the SH3 domain at concentrations expected to ensure >95% peptide was bound (see the Supporting Information). Fourier transform infrared (FT IR) spectra were recorded using a dry N2(g)-purged Agilent Cary 670 FT IR spectrometer with a N2(1)-cooled MCT detector at 2 and 4 cm<sup>-1</sup> resolution. A 4-term Blackman Harris apodization function and zero-filling factor of 8 were applied to process all interferograms, which were averages of 8000 scans. IR absorption spectra of the C-D probes at each proline residue were generated using transmission spectra of unlabeled and labeled peptide complexes acquired under identical conditions. To correct for slowly varying residual background absorbance, a polynomial fit was then subtracted from the spectra. Each background-subtracted absorption spectrum was fit to a Gaussian function or sum of Gaussian functions to determine the number, relative intensities, center frequencies, and full width at half-maximum line widths of the absorption bands (see the Supporting Information). The reported averages and standard deviations were obtained from analysis of spectra of independently prepared samples.

**Isothermal Titration Calorimetry.** ITC experiments were performed at 25 °C using a Nano ITC (TA Instruments). Protein solutions at 500  $\mu$ M to 1.7 mM were titrated with 20–25 additions of peptide solutions of 10 to 20-fold greater concentration. All solutions were prepared in 50 mM sodium phosphate, pH 7.0, 100 mM NaCl. Details are provided in the Supporting Information. All experiments were performed in triplicate.

MD Simulations. MD simulations were performed with the AMBER16 software package<sup>36</sup> and implemented the ff14SB force-field<sup>37,38</sup> and TIP3P model for water molecules.<sup>39</sup> The initial coordinates for the protein–peptide complexes were generated using X-ray crystal structures.<sup>35,40</sup> Addition or changes to residues in the structural models were introduced using Chimera (UCSF). Following equilibration, one 100 ns production trajectory with 2 fs steps was run for each protein–peptide complex and analyzed with CPPTRAJ from AmberTools16.<sup>41</sup> Additional details are provided in the Supporting Information.

# ■ RESULTS AND DISCUSSION

We prepared pNS5A, pPbs2, and p(P(-2,1)A)Pbs2 with  $d_3$ Pro incorporated at each proline residue and used the vibrations of the C-D bonds to characterize each site in the complexes with SH3<sup>Sho1</sup> and/or SH3<sup>Fyn</sup>. The C-D vibrations of  $d_3$ Pro consist of asymmetric and symmetric stretching modes of the C<sub>0</sub>D<sub>2</sub> methylene and the C<sub>0</sub>D stretching mode (Figure 2).<sup>20,22</sup> As observed for the free ligands,<sup>9</sup> the

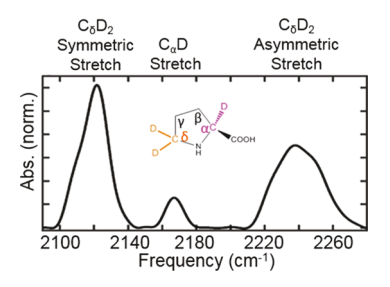


**Figure 2.** FT IR spectrum of  $d_3\text{P3-p}(P(-2,1)\text{A})\text{Pbs2}$  bound to SH3<sup>Sho1</sup> showing absorptions of the three C–D vibrational modes and the structure of  $d_3\text{Pro}$  with the  $C_\delta D_2$  and  $C_\alpha D$  bonds colored orange and magenta, respectively.

complexes with SH3 domains showed absorptions associated with the individual  $C_\delta D_2$  modes with complicated line shapes that revealed the presence of multiple distinct but overlapping bands (Figures 2 & 3). However, the absorptions of the asymmetric and symmetric  $C_\delta D_2$  modes did not vary correspondingly among sites or states of the ligand (Figure S1). As distinct modes with different symmetries, the modes likely differ in their sensitivity to interactions with their environment. Because of this complexity, we currently limit our focus to the analysis and interpretation of the absorption associated with the  $C_\delta D_2$  asymmetric stretch; analysis of the symmetric stretch will be reported in a subsequent publication.

Considering the spectra of all labeled residues of the free ligands and complexes, a total of 28 samples characterized in multiple replicates, we found that the asymmetric  $C_{\delta}D_{2}$ absorptions were best modeled by a superposition of two or three bands (Figure 3, Table 1, Figures S3-S6). Particularly clear examples showing absorption envelopes with three distinguishable features are provided by the spectra for P(-1) and P2 of pNS5A bound to SH3<sup>Fyn</sup> and P3 of pPbs2 bound to SH3<sup>Sho1</sup>. A detailed description of the spectral fitting is given in the Supporting Information and previous publication. The three bands were separated in frequency by  $\sim$ 14 cm<sup>-1</sup> and generally shifted as a set among samples. For ease of discussion, we refer to them in order of increasing frequency as bands and associated spectral subpopulations A, B, and C (Figure 3, Table 1). All spectra showed bands B and C. Band B appeared at a center frequency of 2234–2245 cm<sup>-1</sup> and dominated the spectra with one exception. Band C appeared with lower intensity at frequencies of 2247-2258 cm<sup>-1</sup>. Band A appeared in some but not all spectra at frequencies lower than 2233 cm<sup>-1</sup> and contributed up to 30% of the integrated absorbance. Thus, the spectra of the C-D probes provided evidence for at least three distinct subpopulations. The ubiquitous presence of bands B and C indicated that two are populated by all residues, while the presence of band A depended on the residue and whether a ligand was bound to an SH3 domain.

The variation observed among the spectra for the residues in the SH3 complexes generally reflected the three-fold symmetry of the PPII structure that places residues in comparable local environments (Figure 1b). To aid comparison, the data are arranged in Figures 3–5 to stack the residues according to equivalent locations in the complexes. All of the nonmotif proline residues with side chains expected to point away from the protein surface, P(-1) and P(-

The Journal of Physical Chemistry B

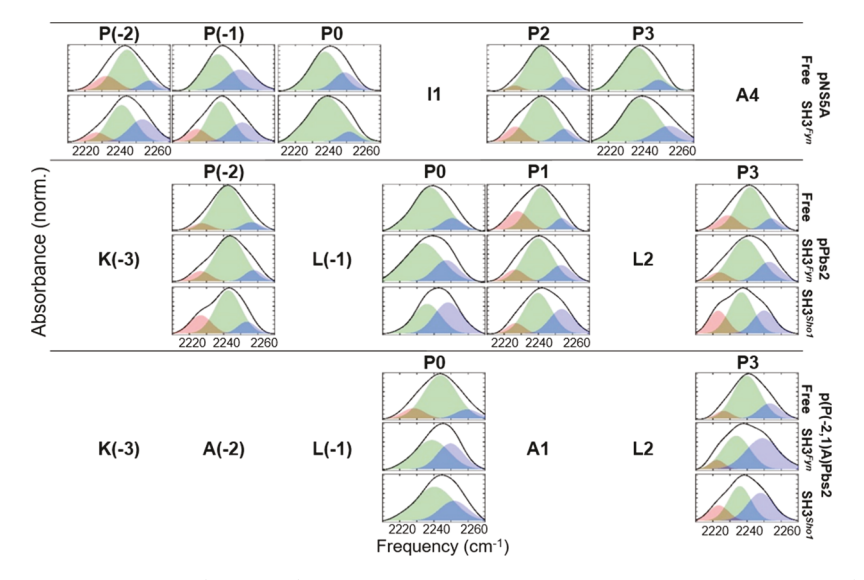


Figure 3.  $C_{\delta}D_2$  asymmetric stretch absorption (black line) for C–D probes incorporated at each proline of pNSSA (top panel), pPbs2 (middle panel), and p(P(-2,1)A)Pbs2 (bottom panel). In each panel, the top rows show spectra for the free ligand, while the middle and bottom rows show spectra for the complexes with SH3 domains. Shown are the average spectra, and the component bands A, B, and C from spectral modeling are colored red, green, and blue, respectively. Spectra of the free ligands were reprinted with permission from ref 9. Copyright 2018 American Chemical Society.

and P3 of pNS5A, with side chains expected to align and pack within grooves of the SH3 domains, both showed solely bands B and C. However, the spectral subpopulations did not correspond for motif residues of pPbs2 or p(P(-2,1)A)Pbs2 as expected from the PPII structure. While P0 showed only bands B and C, band A also appeared for P3. The presence of three rather than two distinct subpopulations at P3 in the SH3 complexes of pPbs2 and p(P(-2,1)A)Pbs2 was unique among the motif residues.

The evidence for three spectral subpopulations is strong; however, establishing confidence in their assignment to specific molecular features can be challenging. An interpretation supported by our prior analysis of the free ligands is that the bands reflect sensitivity of the C-D vibration to the proline backbone conformation. Proline can adopt two stable conformers, referred to as  $\alpha$  and  $\beta$ , differentiated by the  $\psi$  $(C^{\alpha}-C)$  torsional angle. 42,43 The  $\beta$  conformer forms the extended PPII structure, while the  $\alpha$  conformer typically manifests as a kink within the PPII structure and is disfavored for residues that precede proline due to steric hindrance. In our study of the free ligands, band A appeared for all residues not preceding another proline and for those residues that showed population of the  $\alpha$  conformer in MD simulations. Density functional theory calculations of proline when adopting  $\alpha$ conformers yielded a 12 cm<sup>-1</sup> lower frequency for the C<sub>δ</sub>D<sub>2</sub> asymmetric stretch than the  $\beta$  conformer, in excellent agreement with the experiment. Additional support for assignment of band A to adoption of the  $\alpha$  conformer and bands B and C to the  $\beta$  conformer that forms the PPII structure was the observation that heating the PR ligands led to decreased intensity at high frequency and shift of the absorbance envelope to lower frequency, consistent with thermally induced loss of the PPII structure and gain of  $\alpha$ conformer population. Finally, visible CD spectroscopy to probe the global secondary structure of the ligands accorded with the IR spectra and MD simulations in supporting that pNS5A had the greatest PPII content, followed by pPbs2, and

then p(P(-2,1)A)Pbs2, corresponding with their proline content.

Assignment of band A to a subpopulation that adopts the  $\alpha$ conformer of the disordered structure and bands B and C to the  $\beta$  conformer of the PPII structure implies that the ligands in complex with the SH3 domains exist as an ensemble with residue-specific variation in the secondary structures. The motif residues P0 and P3 of pNS5A show two spectral subpopulations exclusively associated with the PPII structure. In comparison, for pPbs2 and p(P(-2,1)A)Pbs2, the motif residue P0 adopts solely the PPII structure, whereas P3 also populates the  $\alpha$  conformer. MD simulations of the PR ligands in the complex with SH3Fyn were consistent with this interpretation, showing population of the  $\alpha$  conformer at P3 but not P0 for both pPbs2 and p(P(-2,1)A)Pbs2 and its absence for both motif residues of pNS5A (Figure S2). Band A also appeared in the spectra of all of the nonmotif, solventexposed proline residues of the ligands in the SH3 complexes. However, in contrast to the motif residues, the nonmotif residues did not sample the  $\alpha$  conformer in the MD simulations. Thus, either a molecular feature other than or in addition to population of the  $\alpha$  conformer is associated with band A, or the MD simulations of the complexes did not fully capture the conformational landscape of the systems. The standard force field employed in the simulations might not sufficiently account for the small energy differences among states needed to recapitulate the IR data.

Assignment of states B and C to molecular features is more ambiguous. We previously had hypothesized that they could reflect two subpopulations of the PPII structure differentiated by the  $\psi$  backbone angle because of the asymmetry of the histograms of  $\psi$  angles from MD simulations of the free ligands. An alternate interpretation is that bands B and C reflect subpopulations of the PPII structure differentiated by the amide backbone solvation. The tertiary amide carbonyl preceding a proline is known to be a strong hydrogen bond donor due to the electron-donating potential of the  $C_\delta$  methylene. Acciprocally, the interaction of the carbonyl

Table 1. Parameters from Modeling of C<sub>δ</sub>D<sub>2</sub> Asymmetric Stretch Absorptions

					C <sub>s</sub> D <sub>s</sub> asymme	tric stretch		
			pNS5A		$C_{\delta}D_2$ asymmetric stretch		p(P(-2,1)A)Pbs2	
			$\nu \text{ (cm}^{-1})$	area (%)	$\frac{\nu \text{ (cm}^{-1})}{\nu \text{ (cm}^{-1})}$	area (%)	$\frac{\nu \text{ (cm}^{-1})}{\nu \text{ (cm}^{-1})}$	area (%)
P(-2)	free	A	$2232.8 \pm 1.0$	24 ± 8	$2226.8 \pm 1.2$	6 ± 4	p (em )	ureu (/0,
1 ( 2)		В	$2244.8 \pm 1.2$	64 ± 8	$2242.4 \pm 0.4$	$85 \pm 6$		
		С	$2257.7 \pm 0.7$	$12 \pm 3$	$2256.7 \pm 1.4$	9 ± 6		
	SH3 <sup>Fyn</sup>	A	$2227.2 \pm 1.4$	12 ± 2	$2226.7 \pm 0.4$	$12 \pm 0.3$		
		В	$2242.1 \pm 0.7$	59 ± 4	$2243.6 \pm 0.4$	$76 \pm 4$		
		С	$2254.6 \pm 0.7$	$29 \pm 3$	$2257.7 \pm 0.4$	12 ± 4		
	SH3 <sup>Sho1</sup>	A			$2226.8 \pm 0.7$	23 ± 4		
		В			$2242.8 \pm 0.5$	$65 \pm 1$		
		С			$2253.6 \pm 1.0$	$12 \pm 3$		
P(-1)	free	A						
		В	$2238.2 \pm 1.2$	$77 \pm 8$				
		С	$2252.5 \pm 1.6$	$23 \pm 8$				
	$SH3^{Fyn}$	A	$2223.6 \pm 0.1$	$11 \pm 5$				
		В	$2238.4 \pm 0.8$	$69 \pm 10$				
		С	$2252.6 \pm 1.1$	$19 \pm 11$				
P0	free	A					$2229.1 \pm 1.4$	$27 \pm 8$
		В	$2237.4 \pm 0.4$	$75 \pm 5$	$2237.6 \pm 0.5$	$84 \pm 8$	$2243.3 \pm 0.8$	$63 \pm 9$
		С	$2249.0 \pm 0.6$	$25 \pm 5$	$2250.6 \pm 1.1$	$16 \pm 8$	$2255.8 \pm 0.7$	$10 \pm 4$
	$SH3^{Fyn}$	A					$2239.2 \pm 1.2$	$62 \pm 5$
		В	$2237.9 \pm 1.3$	$87 \pm 2$	$2234.0 \pm 2.2$	$74 \pm 6$	$2249.8 \pm 0.7$	$38 \pm 5$
		С	$2251.2 \pm 1.1$	$13 \pm 2$	$2247.5 \pm 0.9$	$26 \pm 6$		
	SH3 <sup>Sho1</sup>	A			$2235.2 \pm 1.0$	$42 \pm 9$	$2240.4 \pm 0.9$	$68 \pm 7$
		В			$2247.5 \pm 1.1$	$58 \pm 9$	$2252.0 \pm 1.0$	$32 \pm 7$
		С						
P1	free	A			$2228.0 \pm 0.9$	$24 \pm 3$		
		В			$2241.8 \pm 0.6$	$66 \pm 3$		
		С			$2253.9 \pm 0.2$	$10 \pm 0.3$		
	$SH3^{Fyn}$	A			$2226.3 \pm 0.2$	$13 \pm 1$		
		В			$2239.8 \pm 0.2$	$68 \pm 1$		
		C			$2253.3 \pm 0.4$	$19 \pm 1$		
	SH3 <sup>Sho1</sup>	A			$2226.9 \pm 0.9$	$10 \pm 2$		
		В			$2239.9 \pm 1.3$	$59 \pm 7$		
		C			$2253.8 \pm 0.9$	$31 \pm 7$		
P2	free	A	$2226.4 \pm 0.6$	$4 \pm 1$				
		В	$2241.7 \pm 0.6$	$81 \pm 2$				
		C	$2255.9 \pm 0.5$	$14 \pm 2$				
	SH3 <sup>Fyn</sup>	A	$2226.5 \pm 0.1$	$15 \pm 1$				
		В	$2241.8 \pm 0.3$	$72 \pm 2$				
		C	$2255.5 \pm 0.1$	$12 \pm 1$				
P3	free	A			$2228.4 \pm 0.6$	$12 \pm 3$	$2226.3 \pm 0.8$	$8 \pm 1$
		В	$2237.0 \pm 1.0$	$87 \pm 3$	$2241.7 \pm 0.4$	$75 \pm 3$	$2239.9 \pm 0.6$	$72 \pm 3$
		C	$2249.1 \pm 0.7$	$13 \pm 3$	$2254.4 \pm 0.5$	$14 \pm 2$	$2253.3 \pm 0.8$	$20 \pm 3$
	$SH3^{Fyn}$	A			$2223.1 \pm 0.4$	$8 \pm 1$	$2222.7 \pm 0.5$	$10 \pm 3$
		В	$2237.4 \pm 1.2$	$70 \pm 9$	$2238.3 \pm 0.9$	$66 \pm 4$	$2234.8 \pm 0.3$	$48 \pm 4$
		C	$2253.4 \pm 1.2$	$30 \pm 9$	$2252.3 \pm 0.8$	$26 \pm 4$	$2250.0 \pm 1.7$	$42 \pm 1$
	SH3 <sup>Sho1</sup>	A			$2223.1 \pm 0.4$	$23 \pm 3$	$2222.7 \pm 0.9$	$14 \pm 5$
		В			$2236.7 \pm 0.3$	$51 \pm 5$	$2237.2 \pm 1.0$	$62 \pm 14$
		C			$2250.0 \pm 0.7$	$26 \pm 3$	$2250.2 \pm 1.3$	$23 \pm 9$

with water or other hydrogen bond donors is likely to influence the methylene  $C_\delta D_2$  vibration. Another possible contributor is an interaction with the imino lone pair. Additionally, although the spectra provide evidence for at least three distinct subpopulations, more states with degenerate frequencies could exist. Unfortunately, analysis of the MD simulations of the complexes did not provide clear evidence to help evaluate these possible interpretations. A combination of additional experimental and computational studies with systematically

varying sequences are being pursued to enable a more definitive interpretation.

So far, the experimental and computational analyses reasonably support a minimal model consisting of an ensemble of two subpopulations with the PPII structure (associated with bands B and C), possibly differentiated by small backbone angular distributions or hydration and a subpopulation adopting the  $\alpha$  conformer (associated with band A). All experimental and computational data for the free ligands and

The Journal of Physical Chemistry B

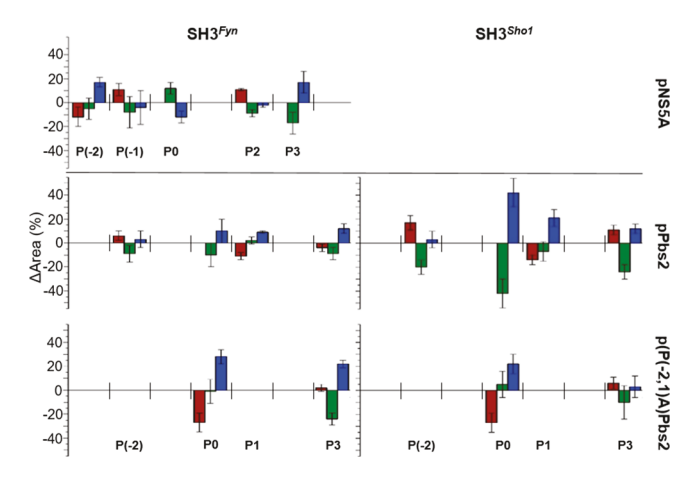


**Figure 4.** Changes in the relative integrated absorbance of band A (red bars), band B (green bars), and band C (blue bars) upon association of the PR ligands with SH3<sup>Fyn</sup> (left) and SH3<sup>Sho1</sup> (right). Error calculated from propagation.

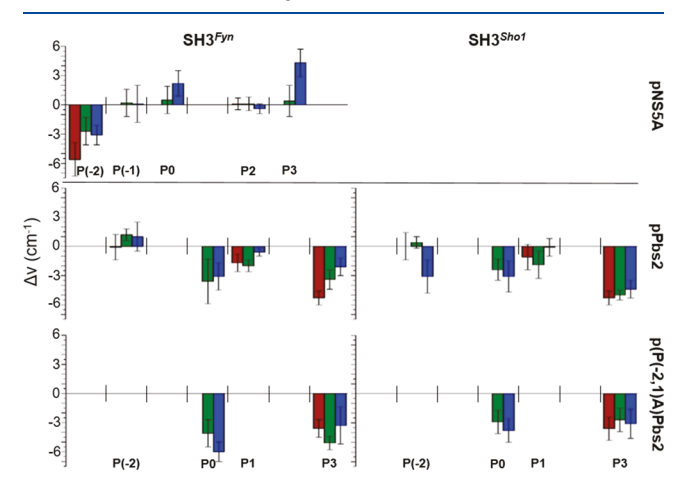


**Figure 5.** Changes in the frequency of the  $C_\delta D_2$  asymmetric stretch band A (red), band B (green), and band C (blue) induced upon association of the PR ligands with SH3<sup>Fyn</sup> (left) and SH3<sup>Sho1</sup> (right). Error calculated from propagation.

motif residues of the complexes support that band A is associated with the  $\alpha$  conformer, giving reasonable confidence in the assignment. However, band A appears for all nonmotif residues for the SH3 complexes, but the  $\alpha$  conformer is not sampled in MD simulations, raising the possibility that the subpopulation has an alternate molecular basis for those sites.

The spectra of the complexes mostly reflected the relationships between residues arising from the symmetry of the ligands' overall PPII structure. However, differences in the binding-induced changes in the spectral subpopulations indicate unique binding mechanisms. These differences arise in part from the distinct spectra at P3 of pNSSA compared to pPbs2 and p(P(-2,1)A)Pbs2, but even more so from variation among the free ligands. Most frequently, binding led to an increase in subpopulation C and a decrease in B, suggesting a shift of the ensemble between states associated with the PPII structure, whereas the changes in subpopulation A were comparably more variable.

For pNS5A, in the free-state, the four proline residues of the motif and flanking sites adopted only the two subpopulations associated with the PPII structure. For the motif proline residues, binding SH3<sup>Fyn</sup> resulted in transfer between the PPII

subpopulations. For the nonmotif, solvent-directed residues, binding also led to a gain of subpopulation A. Therefore, whether or not associated with the  $\alpha$  conformer, complexation induced a new subpopulation at the solvent-directed sites in pNS5A.

As observed for pNS5A, binding of pPbs2 with SH3<sup>Fyn</sup> induced significant changes at the motif proline residues solely in the contributions of spectral subpopulations B and C associated with the PPII structure. Subpopulation A, however, was present at P3 in both the free-state and SH3<sup>Fyn</sup> complex. The nonmotif residue P(-2) of pPbs2, such as the structurally related nonmotif residues P(-1) and P2 of pNS5A, gained subpopulation A upon complexation. In contrast, the nonmotif residue P1 of pPbs2 displayed a net decrease in subpopulation A. The contribution of subpopulation A was similar among the related nonmotif residues in the complexes, but P1 of pPbs2 showed greater population in the free ligand. Interestingly, the changes to the spectra for pPbs2 arising from complexation with SH3<sup>Sho1</sup> were qualitatively the same as SH3<sup>Fyn</sup>, but the magnitude of the impact was greater when binding SH3<sup>Sho1</sup>. Another distinction was that binding to SH3<sup>Sho1</sup>, unlike SH3<sup>Fyn</sup>. led to gain of subpopulation A at P3.

The spectral subpopulations observed for p(P(-2,1)A)Pbs2in the SH3 complexes generally matched those of pPbs2, and many of the changes induced by association were qualitatively similar for the residues of the related ligands. A striking exception was the substantial decrease in subpopulation A at P0 of p(P(-2,1)A)Pbs2 upon binding either SH3 domain. Uniquely among the ligands, subpopulation A appeared at the residue for the free ligand p(P(-2,1)A)Pbs2 but then disappeared in the complexes with both SH3 domains. Correlating with the changes in band A in the experimental spectra, the  $\alpha$  conformer was populated by P0 in MD simulations of free p(P(-2,1)A)Pbs2 but not in the  $SH3^{Fyn}$ complex. Together, the experimental and computational data suggest that the mutation of pPbs2 induced a population of the non-PPII structure at motif residue P0, but the population then converted to the PPII structure upon complexation with SH3 domains.

Like the number and contribution of bands, the center frequencies reported on the varied local environments of the residues and their distinct involvement in the complexation of the ligands and SH3 domains (Table 1, Figure 5). For the free ligands, the frequencies of the set of bands for a proline residue compared to the other residues within the sequence correlated with whether another proline followed, similarly as the presence of band A, demonstrating the sensitivity to local structure and environment. Association with the SH3 domains impacted the frequencies of the residues disparately, although the binding-induced shifts were always smaller than the frequency separation between the component bands. As for the band subpopulations, the changes in the frequencies for the residues corresponded with the relationships between their local environments in the complexes. Specifically, the frequencies for the nonmotif residues expected to be solventexposed in the complexes were either insensitive (pNS5A) or less sensitive than the motif-residues (pPbs2) to binding, whereas the frequencies for the motif residues that pack against the SH3 domain were impacted more substantially. While the sensitivity of the frequencies among the residues of a ligand reflected the ligands' PPII symmetry, among all sites, the relative magnitude and direction of the changes correlated with whether the ligand was type I or II. For type I ligands, pPbs2

and p(P(-2,1)A)Pbs2, the shifts in the frequencies were overall greater in magnitude and always toward lower energy. Also notable is that the patterns in the changes for the two type I ligands were similar along the ligand sequences and for their association with the two SH3 domains. In contrast, for the type II ligand pNS5A, the frequency of only band C of motif residues P0 and P3 was affected by binding, and the band conversely shifted to higher frequency. The opposite behavior found for the type I and II ligands likely reflects their opposite binding orientations. An orientation-dependent interaction with the SH3 domain surface could engender such disparate frequency perturbations. P(-2) of pNS5A, which has no corresponding proline residue in the other ligands, was an outlier. The band structure for this residue was similar to the motif-flanking residues for the SH3<sup>Fyn</sup> complexes. However, for the free ligand, band A was substantially higher in frequency compared to those likewise assigned for the other residues. Additionally, binding to SH3Fyn shifted the set of bands to lower frequencies, distinct from other residues of pNS5A.

As a set, the frequencies of the component bands did vary among the residues in sensitivity to binding. However, the variation among sites and conditions never neared the frequency separation between component bands, and moreover, the component bands typically were all affected similarly as a set. Thus, the magnitude of the frequency changes does not strongly argue for the appearance of fundamentally distinct states upon complexation. Although additional subpopulations with degenerate frequencies could and likely exist, three states are consistent with the simplest, conservative interpretation of the data. Assuming three states, the spectra indicate that association of the ligand with the SH3 domains results in redistribution among the subpopulations, while in some cases, perturbing the local environments sufficiently to affect the vibrational frequencies of the IR bands. The observed shifting among the set of subpopulations as a result of the ligandprotein binding evokes the picture of a conformational selection mechanism, in which complexation alters the populations of pre-existing states. 46,47

The spectra of the SH3 complexes were qualitatively the same for pPbs2 and the mutated sequence p(P(-2,1)A)Pbs2, suggesting similar binding modes. However, a key difference between the ligands was seen in their sensitivity to binding SH3<sup>Sho1</sup> compared to SH3<sup>Fyn</sup>. In particular, the spectra for pPbs2 were more greatly impacted upon association with the physiologically relevant partner SH3<sup>Sho1</sup> than SH3<sup>Fyn</sup> (Figure 6a,b), while the differences between the SH3 complexes for

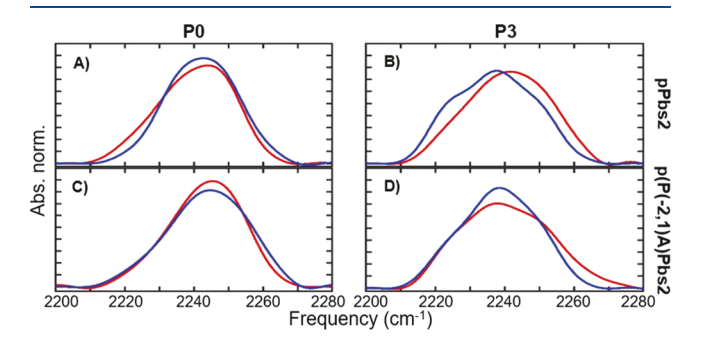


**Figure 6.** FT IR spectra of the  $C_\delta D_2$  asymmetric stretch of P0 (A) and P3 (B) for pPbs2 (top row) and P0 (C) and P3 (D) for p(P(-2,1)A)Pbs2 (bottom row) bound to SH3<sup>Fyn</sup> (red line) and SH3<sup>Sho1</sup> (blue line). Shown are the average spectra.

p(P(-2,1)A)Pbs2 were comparably minor (Figure 6c,d). Thus p(P(-2,1)A)Pbs2 appeared to adapt its structure to similarly recognize the different SH3 domains, whereas the changes induced in pPbs2 depended more on the specific binding partner. Unlike pPbs2, p(P(-2,1)A)Pbs2 displays recognition promiscuity among the yeast SH3 domains in vitro assays, and introduction of the mutations into Pbs2 leads to in vivo fitness defects.<sup>34</sup> The greater adaptability of p(P(-2,1)A)Pbs2 when interacting with different partners likely facilitates the crossreactivity amongst yeast SH3 domains. This mechanism supplements a prevalent view that the charged residues outside the PR motif itself mediate specificity, 25 which do not differ between pPbs2 and p(P(-2,1)A)Pbs2, and argues that the conformational freedom dictated by the sequence encompassing the PR motif also plays a role. Conformational flexibility has been similarly evoked to explain binding promiscuity for other disordered and structured proteins.48-<sup>52</sup> In a broader context, tailoring conformational flexibility of proteins following gene duplication is proposed as a mechanism for evolution of new, specific functions.<sup>52</sup> The ability to detect and measure the ensemble of states adopted by protein sequences enables better experimental elucidation of such models.

To assess the potential relationship between the bindinginduced changes in the PR ligand ensembles and the binding thermodynamics, we characterized the binding interactions via ITC (Table 2). As anticipated, pPbs2 and p(P(-2,1)A)Pbs2

Table 2. Thermodynamic Parameters for Binding of the PR Ligand to the SH3 Domain

ligand	$K_{\mathrm{D}} \; (\mu \mathrm{M})$	$\Delta H$ (kJ mol <sup>-1</sup> )	$-T\Delta S$ (kJ mol <sup>-1</sup> )								
SH3 <sup>Fyn</sup>											
pNS5A <sup>a</sup>	0.62	-41.0	5.0								
pPbs2	$23.9 \pm 0.2$	$-35.4 \pm 0.1$	$9.0 \pm 1.0$								
p(P(-2,1)A)Pbs2	$70.0 \pm 2.8$	$-42.0 \pm 1.9$	$18.3 \pm 1.9$								
	SH	13 <sup>Sho1</sup>									
pPbs2	$3.4 \pm 0.3$	$-28.2 \pm 0.2$	$-2.5 \pm 0.1$								
p(P(-2,1)A)Pbs2	$15.7 \pm 0.8$	$-38.1 \pm 0.3$	$10.6 \pm 0.3$								
<sup>a</sup> Ref 35.											

showed higher affinity for the cognate partner SH3<sup>Sho1</sup> than SH3<sup>Fyn</sup>. Notably, for both SH3 domains, the mutation of the proline residues to alanine decreased affinity. Moreover, in both cases, the mutations led to a similar substantial penalty to the entropy of binding. The unfavorable entropy contribution is in line with the effect of the mutations on the ligand's populated states. Mutation of pPbs2 to generate p(P(-2,1)-A)Pbs2 induced at P0 in the free ligand the appearance of subpopulation A that is reasonably assigned to adoption of the  $\alpha$  conformer, indicative of the non-PPII structure. Upon complexation with either the SH3 domain, the subpopulation A at P0 of p(P(-2,1)A)Pbs2 disappeared, or rather the spectra reflected only subpopulations associated with the PPII structure, similarly as pPbs2. Altogether, the data suggest that the mutations led to a new subpopulation at P0 of p(P(-2,1)A)Pbs2, increasing the heterogeneity of the ensemble in comparison to pPbs2. This engendered the need for greater conformational restriction upon complexation and resulted in the entropy penalty shown in the thermodynamic analysis.

The changes in subpopulation A were also consistent with other differences among the ligands in the relative entropies of binding with the SH3 domains. For example, the appearance of

subpopulation A induced at both the nonmotif residues P(-1)and P(2) of pNS5A upon complexation with SH3<sup>Fyn</sup> reflects gain of new distinct subpopulations in the ensemble and thus an increase in the heterogeneity of total populated states, which should contribute to the favorable binding entropy. In comparison, for pPbs2 association with SH3<sup>Fyn</sup>, subpopulation A increases for one but not the other of the analogous nonmotif residues, corresponding with the comparably less favorable binding entropy. Other observations supporting a relationship between changes in subpopulation A and binding entropy were its growth at P3 of pPbs2 upon association with SH3<sup>Sho1</sup> but not SH3<sup>Fyn</sup>, as well as the larger growth at P(-2), correlating with the more favorable entropy change for binding SH3<sup>Sho1</sup> than SH3<sup>Fyn</sup>. We note, however, that these states do not account for the whole system, and the states populated by the unlabelled residues and the residues of the SH3 domains, which were not accessed in this study, are also likely to contribute to the thermodynamics. Indeed, previous NMR relaxation studies suggest that the dynamics of the side chains of proteins such as the SH3 domain are likely to contribute significantly to binding entropy.<sup>3</sup> Nevertheless, the data support that the dynamic ensemble of the ligand captured by the approach plays a role in the binding thermodynamics.

Prior CD spectroscopy, thermodynamic analysis and computational studies of PR ligands have established that structural preorganization to minimize the conformational restriction necessary for complex formation can promote binding of flexible sequences through reduction of unfavorable entropy changes. 53,54 Disordered sequences in general often show the preformed structure resembling their final conformational state in a complex. Complicating the picture, however, is that sequences also typically contain mixtures of local regions with strong or weak conformational preferences. 55-57 Conversely, some sequences remain disordered when in complex with their targets.<sup>58</sup> This study provides experimental support for the prevailing models but importantly affords unique insights into local dynamics and their involvement in molecular recognition. For instance, even when the ligands are bound to SH3 domains, the IR spectra indicated that all residues populate an ensemble of states. Motif residue P3 of p(P(-2,1)A)Pbs2 and pPbs2 displayed particularly high heterogeneity, showing three subpopulations in both free and bound states. In addition, beyond uncovering that the mutation of pPbs2 to p(P(-2,1)A)Pbs2 disrupted the preorganization of the PPII structure for binding, the perturbation was shown to be relatively localized to P0, with only minor impact at P3. The localized influence of the mutations is in agreement with previous host—guest studies of peptide sequence and structure. 59,60 Furthermore, the changes in the IR spectra of the nonmotif residues of pNS5A revealed localized gain in the number of subpopulations upon complexation which could contribute favorably to entropy changes and thereby promote association. These local changes could be considered a subtle incidence of more extreme cases of "cryptic disorder" in molecular recognition, such as found for BCL-xL with its partner PUMA, wherein association induces partial unfolding.61,62

## CONCLUSIONS

We applied IR spectroscopy using C-D vibrational probes as a nonperturbative experimental approach with high temporal resolution to measure the dynamics of PR ligands with residue-specific detail and elucidate their involvement in recognition of

SH3 domains. The three bands observed in the IR spectra of the C–D probes provided evidence for three underlying subpopulations that depended on the residue probed and its association with SH3 domains. Previous characterization of the same bonds via NMR spectroscopy found the subpopulations to be in rapid exchange, indicating that the ensemble captured by IR spectroscopy is highly dynamic.<sup>22</sup>

The functional contribution of such small-scale, rapidly interconverting states is not well understood. While not necessarily the case for all rapid motions, this study provides evidence that the dynamic ensemble detected by IR spectroscopy is functionally important. We believe that the spectral subpopulations reflect small-scale differences in backbone conformers or hydrogen bonding that responds to binding SH3 domains in distinct ways within the different PR sequences, providing evidence for unique binding mechanisms. The disparity in adaptability upon binding suggested by the C-D probes in p(P(-2,1)A)Pbs2 and pPbs2 corresponds with their distinct specificities in recognition of SH3 domains. In addition, changes in the ensembles of subpopulations uncovered in the PR ligands induced upon association with SH3 domains provide a consistent molecular basis for differences in binding entropy. Generally, the disparity in spectral features among the PR ligands was greater than found between the same ligand bound to different SH3 domains, indicating that the nature of the ligand sequence rather than the SH3 domain they bind more strongly determines the binding mechanism. Additionally, the data suggested that the binding mechanisms of the ligands differ more predominantly as a result of variation in the free ligand ensembles, indicating that the dynamic free states of disordered sequences are key to understanding their recognition.

Investigation of additional PR ligands with systematic variation in sequence along with better modeling of the complexes will further inform on the relationship between the protein sequence and structural dynamics and how the conformational landscape influences the recognition of SH3 domains. Work is also in progress to probe the interaction from the perspective of the SH3 domain with C-D and other vibrational probes to provide more comprehensive insight into the relationship between changes in conformational heterogeneity, entropy, and specificity.<sup>63</sup> PR sequences are abundant in eukaryotic proteomes, serving as recognition elements for binding partners besides SH3 domains as well as performing other functions, <sup>24,25,45,64</sup> but investigating such intrinsically disordered and conformationally dynamic sequences has been difficult. The ability of IR spectroscopy to capture even the most rapidly interconverting states, combined with the residuespecific precision provided by C-D probes, should afford new information to advance our understanding of these elusive but critical parts of proteins.

# ASSOCIATED CONTENT

# S Supporting Information

The Supporting Information is available free of charge on the ACS Publications website at DOI: 10.1021/acs.jpcb.9b07036.

Experimental details of protein expression and purification, ITC, MD simulations, and sample preparation; and evaluation of fits of spectra (PDF)

#### AUTHOR INFORMATION

## **Corresponding Author**

\*E-mail: thielges@indiana.edu.

#### ORCID ®

Megan C. Thielges: 0000-0002-4520-6673

#### **Author Contributions**

All authors have given approval to the final version of the manuscript.

#### **Notes**

The authors declare no competing financial interest.

#### ACKNOWLEDGMENTS

G.S.B., R.E.H., and M.C.T. thank Indiana University and the National Science Foundation (grant no. MCB-1552996) for funding. R.E.H. was also supported by the Graduate Training Program in Quantitative and Chemical Biology (T32 GM109825).

#### REFERENCES

- (1) Oldfield, C. J.; Dunker, A. K. Intrinsically Disordered Proteins and Intrinsically Disordered Protein Pegions. Annu. Rev. Biochem. 2014, 83, 553-584.
- (2) Wright, P. E.; Dyson, H. J. Intrinsically Disordered Proteins in Cellular Signalling and Regulation. Nat. Rev. Mol. Cell Biol. 2015, 16,
- (3) Caro, J. A.; Harpole, K. W.; Kasinath, V.; Lim, J.; Granja, J.; Valentine, K. G.; Sharp, K. A.; Wand, A. J. Entropy in Molecular Recognition by Proteins. Proc. Natl. Acad. Sci. U.S.A. 2017, 114, 6563-6568.
- (4) Jensen, M. R.; Ruigrok, R. W.; Blackledge, M. Describing Intrinsically Disordered Proteins at Atomic Resolution by NMR. Curr. Opin. Struct. Biol. 2013, 23, 426-435.
- (5) Kosol, S.; Contreras-Martos, S.; Cedeño, C.; Tompa, P. Structural Characterization of Intrinsically Disordered Proteins by NMR spectroscopy. Molecules 2013, 18, 10802-10828.
- (6) Uversky, V. N.; Dunker, A. K. Intrinsically Disordered Protein Analysis 1; Humana: New York, 2012; Vol. 895.
- (7) Uversky, V. N.; Dunker, A. K. Intrinsically Disordered Protein Analysis 2; Humana: New York, 2012; Vol. 396.
- (8) Kikhney, A. G.; Svergun, D. I. A Practical Guide to Small Angle X-Ray Scattering (SAXS) of Flexible and Intrinsically Disordered Proteins. FEBS Lett. 2015, 589, 2570-2577.
- (9) Bukowski, G. S.; Thielges, M. C. Residue-Specific Conformational Heterogeneity of Proline-Rich Sequences Uncovered via Infrared Spectroscopy. Anal. Chem. 2018, 90, 14355-14362.
- (10) Kim, H.; Cho, M. Infrared Probes for Studying the Structure and Dynamics of Biomolecules. Chem. Rev. 2013, 113, 5817-5847.
- (11) Adhikary, R.; Zimmermann, J.; Romesberg, F. E. Transparent Window Vibrational Probes for the Characterization of Proteins with High Structural and Temporal Resolution. Chem. Rev. 2017, 117,
- (12) Ramos, S.; Thielges, M. C. Site-Specific 1D and 2D IR Spectroscopy to Characterize the Conformations and Dynamics of Protein Molecular Recognition. J. Phys. Chem. B 2019, 123, 3551-
- (13) Getahun, Z.; Huang, C.-Y.; Wang, T.; De León, B.; DeGrado, W. F.; Gai, F. Using Nitrile-Derivitized Amino Acids as Infrared Probes of Local Environments. J. Am. Chem. Soc. 2003, 125, 405-411.
- (14) Oh, K.-I.; Lee, J.-H.; Joo, C.; Han, H.; Cho, M. Beta-Azidoalanine as an IR Probe: Application to Amyloid Abeta (16-22) Aggregation. J. Phys. Chem. B 2008, 112, 10352-10357.
- (15) Taskent-Sezgin, H.; Chung, J.; Banerjee, P. S.; Nagarajan, S.; Dyer, R. B.; Carrico, I.; Raleigh, D. P. Azidohomoalanine: A Conformationally Sensitive IR Probe of Protein Folding, Protein Structure, and Electrostatics. Angew. Chem., Int. Ed. Engl. 2010, 49, 7473-7475.

- (16) McMahon, H. A.; Alfieri, K. N.; Clark, K. A. A.; Londergan, C. H. Cyanylated Cysteine: A Covalently Attached Vibrational Probe of Protein-Lipid Contacts. J. Phys. Chem. Lett. 2010, 1, 850-855.
- (17) Chin, J. K.; Jimenez, R.; Romesberg, F. E. Direct Observation of Protein Vibrations by Selective Incorporation of Spectroscopically Observable Carbon-Deuterium Bonds in Cytochrome c. J. Am. Chem. Soc. 2001, 123, 2426-2427.
- (18) Thielges, M. C.; Case, D. A.; Romesberg, F. E. Carbon-Deuterium Bonds as Probes of Dihydrofolate Reductase. J. Am. Chem. Soc. 2008, 130, 6597-6603.
- (19) Sagle, L. B.; Zimmermann, J.; Dawson, P. E.; Romesberg, F. E. A High-Resolution Probe of Protein Folding. J. Am. Chem. Soc. 2004, 126, 3384-3385.
- (20) Adhikary, R.; Zimmermann, J.; Liu, J.; Forrest, R. P.; Janicki, T. D.; Dawson, P. E.; Corcelli, S. A.; Romesberg, F. E. Evidence of an Unusual N-H···N Hydrogen Bond in Proteins. J. Am. Chem. Soc. 2014, 136, 13474-13477.
- (21) Le Sueur, A. L.; Schaugaard, R. N.; Baik, M.-H.; Thielges, M. C. Methionine Ligand Interaction in a Blue Copper Protein Characterized by Site-Selective Infrared Spectroscopy. J. Am. Chem. Soc. 2016, 138, 7187-7193.
- (22) Horness, R. E.; Basom, E. J.; Mayer, J. P.; Thielges, M. C. Resolution of Site-Specific Conformational Heterogeneity in Proline-Rich Molecular Recognition by Src Homology 3 Domains. J. Am. Chem. Soc. 2016, 138, 1130-1133.
- (23) Zarrinpar, A.; Bhattacharyya, R. P.; Lim, W. A.; Gough, N. R. The Structure and Function of Proline Recognition Domains. Sci. Signal. 2003, 2003, tr1.
- (24) Ball, L. J.; Kühne, R.; Schneider-Mergener, J.; Oschkinat, H. Recognition of Proline-Rich Motifs by Protein-Protein-Interaction Domains. Angew. Chem., Int. Ed. Engl. 2005, 44, 2852-2869.
- (25) Li, S. S.-C. Specificity and Versatility of SH3 and Other Proline-Recognition Domains: Structural Basis and Implications for Cellular Signal Transduction. Biochem. J. 2005, 390, 641-653.
- (26) Mayer, B. J. SH3 Domains: Complexity in Moderation. J. Cell Sci. 2001, 114, 1253-1263.
- (27) Fuxreiter, M.; Tompa, P.; Simon, I. Local Structural Disorder Imparts Plasticity on Linear Motifs. *Bioinformatics* **2007**, 23, 950–956.
- (28) Tompa, P.; Schad, E.; Tantos, A.; Kalmar, L. Intrinsically Disordered Proteins: Emerging Interaction Specialists. Curr. Opin. Struct. Biol. 2015, 35, 49-59.
- (29) Yu, H.; Chen, J. K.; Feng, S.; Dalgarno, D. C.; Brauer, A. W.; Schrelber, S. L. Structural Basis for the Binding of Proline-Rich Peptides to SH3 Domains. Cell 1994, 76, 933-945.
- (30) Feng, S.; Chen, J.; Yu, H.; Simon, J.; Schreiber, S. Two Binding Orientations for Peptides to the Src SH3 Domain: Development of a General Model for SH3-Ligand Interactions. Science 1994, 266, 1241 - 1247.
- (31) Ferreon, J. C.; Hilser, V. J. Thermodynamics of Binding to SH3 Domains: The Energetic Impact of Polyproline II (P-II) Helix Formation. Biochemistry 2004, 43, 7787-7797.
- (32) Bhatt, V. S.; Zeng, D.; Krieger, I.; Sacchettini, J. C.; Cho, J.-H. Binding Mechanism of the N-Terminal SH3 Domain of CrkII and Proline-Rich Motifs in cAbl. Biophys. J. 2016, 110, 2630-2641.
- (33) Zeng, D.; Shen, Q.; Cho, J.-H. Thermodynamic Contribution of Backbone Conformational Entropy in the Binding between SH3 Domain and Proline-Rich Motif. Biochem. Biophys. Res. Commun. 2017, 484, 21-26.
- (34) Zarrinpar, A.; Park, S.-H.; Lim, W. A. Optimization of Specificity in a Cellular Protein Interaction Network by Negative Selection. Nature 2003, 426, 676-680.
- (35) Martin-Garcia, J. M.; Luque, I.; Ruiz-Sanz, J.; Camara-Artigas, A. The Promiscuous Binding of the Fyn SH3 Domain to a Peptide from the NS5A Protein. Acta Crystallogr., Sect. D: Biol. Crystallogr. 2012, 68, 1030-1040.
- (36) Case, D. A.; Betz, R. M.; Cerutti, D. S.; Cheatham, T. E., III; Darden, T. A.; Duke, R. E.; Giese, T. J.; Gohlke, H.; Goetz, A. W.; Homeyer, N.; et al. AMBER 2016; University of California: San Francisco, 2016.

- (37) Price, D. J.; Brooks, C. L. A Modified TIP3P Water Potential for Simulation with Ewald Summation. *J. Chem. Phys.* **2004**, *121*, 10096–10103.
- (38) Maier, J. A.; Martinez, C.; Kasavajhala, K.; Wickstrom, L.; Hauser, K. E.; Simmerling, C. ff14SB: Improving the Accuracy of Protein Side Chain and Backbone Parameters from ff99SB. *J. Chem. Theory Comput.* **2015**, *11*, 3696–3713.
- (39) Jorgensen, W. L.; Chandrasekhar, J.; Madura, J. D.; Impey, R. W.; Klein, M. L. Comparison of Simple Potential Functions for Simulating Liquid Water. *J. Chem. Phys.* **1983**, *79*, 926–935.
- (40) Camara-Artigas, A.; Ortiz-Salmeron, E.; Andujar-Sánchez, M.; Bacarizo, J.; Martin-Garcia, J. M. The Role of Water Molecules in the Binding of Class I and II Peptides to the SH3 Domain of the Fyn Tyrosine Kinase. *Acta Crystallogr., Sect. F: Struct. Biol. Commun.* **2016**, 72, 707–712.
- (41) Roe, D. R.; Cheatham, T. E., III PTRAJ and CPPPTRAJ: Software for Processing and Analysis of Molecular Dynamics Trajectory Data. *J. Chem. Theory Comput.* **2013**, *9*, 3084–3095.
- (42) Schimmel, P. R.; Flory, P. J. Conformational Energies and Configurational Statistics of Copolypeptides Containing L-Proline. *J. Mol. Biol.* **1968**, *34*, 105–120.
- (43) MacArthur, M. W.; Thornton, J. M. Influence of Proline Residues on Protein Conformation. *J. Mol. Biol.* **1991**, 218, 397–412.
- (44) Shi, Z.; Olson, C. A.; Rose, G. D.; Baldwin, R. L.; Kallenbach, N. R. Polyproline II Structure in a Sequence of Seven Alanine Residues. *Proc. Natl. Acad. Sci. U.S.A.* **2002**, *99*, 9190–9195.
- (45) Williamson, M. P. The Structure and Function of Proline-Rich Regions in Proteins. *Biochem. J.* **1994**, 297, 249–260.
- (46) Foote, J.; Milstein, C. Conformational Isomerism and the Diversity of Antibodies. *Proc. Natl. Acad. Sci. U.S.A.* **1994**, *91*, 10370–10374
- (47) Zhou, H.-X. From Induced Fit to Conformational Selection: A Continuum of Binding Mechanism Controlled by the Timescale of Conformational Transitions. *Biophys. J.* **2010**, *98*, L15–L17.
- (48) Boehr, D. D.; Nussinov, R.; Wright, P. E. The Role of Dynamic Conformational Ensembles in Biomolecular Recognition. *Nat. Chem. Biol.* **2009**, *5*, 789–796.
- (49) Zhang, Y.; Appleton, B. A.; Wiesmann, C.; Lau, T.; Costa, M.; Hannoush, R. N.; Sidhu, S. S. Inhibition of Wnt Signaling by Dishevelled PDZ Peptides. *Nat. Chem. Biol.* **2009**, *5*, 217–219.
- (50) Alhindi, T.; Zhang, Z.; Ruelens, P.; Coenen, H.; Degroote, H.; Iraci, N.; Geuten, K. Protein Interaction Evolution from Promiscuity to Specificity with Reduced Flexibility in an Increasingly Complex Network. Sci. Rep. 2017, 7, 44948.
- (51) Zimmermann, J.; Oakman, E. L.; Shi, X.; Abbyad, P.; Brooks, C. L.; Boxer, S. G.; Romesberg, F. E. Antibody Evolution Constrains Conformational Heterogeneity by Tailoring Protein Dynamics. *Proc. Natl. Acad. Sci. U.S.A.* **2006**, *103*, 13722–13727.
- (52) James, L. C.; Tawfik, D. S. Conformational Diversity and Protein Evolution: A 60-Year-Old Hypothesis Revisited. *Trends Biochem. Sci.* **2003**, 28, 361–368.
- (53) Ferreon, J. C.; Hilser, V. J. The Effect of the Polyproline II (PPII) Conformation on the Denatured State Entropy. *Protein Sci.* **2003**, *12*, 447–457.
- (54) Zhou, P.; Hou, S.; Bai, Z.; Li, Z.; Wang, H.; Chen, Z.; Meng, Y. Disrupting the Intramolecular Interaction between Proto-Oncogene c-Src SH3 Domain and Its Self-Binding Peptide PPII with Rationally Designed Peptide Ligands. *Artif. Cells, Nanomed., Biotechnol.* **2018**, 46, 1122–1131.
- (55) Fuxreiter, M.; Simon, I.; Friedrich, P.; Tompa, P. Preformed Structural Elements Feature in Partner Recognition by Intrinsically Unstructured Proteins. *J. Mol. Biol.* **2004**, 338, 1015–1026.
- (56) Iešmantavičius, V.; Dogan, J.; Jemth, P.; Teilum, K.; Kjaergaard, M. Helical Propensity in an Intrinsically Disordered Protein Accelerates Ligand Binding. *Angew. Chem., Int. Ed.* **2014**, 53, 1548–1551.
- (57) Arai, M.; Sugase, K.; Dyson, H. J.; Wright, P. E. Conformational Propensities of Intrinsically Disordered Proteins Influence the

- Mechanism of Binding and Folding. Proc. Natl. Acad. Sci. U.S.A. 2015, 112, 9614–9619.
- (58) Tompa, P.; Fuxreiter, M. Fuzzy Complexes: Polymorphism and Structural Disorder in Protein-Protein Interactions. *Trends Biochem. Sci.* **2008**, 33, 2–8.
- (59) Creamer, T. P. Left-Handed Polyproline II Helix Formation is (Very) Locally Driven. *Proteins* **1998**, 33, 218–226.
- (60) Kelly, M. A.; Chellgren, B. W.; Rucker, A. L.; Troutman, J. M.; Fried, M. G.; Miller, A.-F.; Creamer, T. P. Host-Guest Study of Left-Handed Polyproline II Helix Formation. *Biochemistry* **2001**, *40*, 14376–14383.
- (61) Follis, A. V.; Chipuk, J. E.; Fisher, J. C.; Yun, M.-K.; Grace, C. R.; Nourse, A.; Baran, K.; Ou, L.; Min, L.; White, S. W.; et al. PUMA Binding Induces Partial Unfolding within BCL-xL to Disrupt p53 Binding and Promote Apoptosis. *Nat. Chem. Biol.* **2013**, *9*, 163–168.
- (62) Jakob, U.; Kriwacki, R.; Uversky, V. N. Conditionally and Transiently Disordered Proteins: Awakening Cryptic Disorder to Regulate Protein Function. *Chem. Rev.* **2014**, *114*, 6779–6805.
- (63) Ramos, S.; Horness, R. E.; Collins, J. A.; Haak, D.; Thielges, M. C. Site-Specific 2D IR Spectroscopy: A General Approach for the Characteriztion of Protein Dynamics with High Spatial and Temporal Resolution. *Phys. Chem. Chem. Phys.* **2019**, 21, 780–781.
- (64) Kay, B. K.; Williamson, M. P.; Sudol, M. The Importance of Being Proline: The Interaction of Proline-Rich Motifs in Signaling Proteins with Their Cognate Domains. *FASEB J.* **2000**, *14*, 231–241.